CNS & Neurological Disorders - Drug Targets, 2018, *17*, 389-399

RESEARCH ARTICLE

Oleanolic Acid Ameliorates $A\beta_{25-35}$ Injection-induced Memory Deficit in Alzheimer's Disease Model Rats by Maintaining Synaptic Plasticity

Kai Wang[1#], Weiming Sun[1#], Linlin Zhang[2#], Wei Guo[2], Jiachun Xu[1], Shuang Liu[2], Zhen Zhou[2] and Yulian Zhang[2*]

[1]*Graduate Institutes, Tianjin University of Traditional Chinese Medicine, Tianjin, 300193, China;* [2]*Department of Neurology, the Second Hospital Affiliated to Tianjin University of Traditional Chinese Medicine, Tianjin, 300150, China*

Abstract: ***Background***: Abnormal amyloid β (Aβ) accumulation and deposition in the hippocampus is an essential process in Alzheimer's disease (AD).

Objective: To investigate whether Oleanolic acid (OA) could improve memory deficit in AD model and its possible mechanism.

Methods: Forty-five SD rats were randomly divided into sham operation group, model group, and OA group. AD models by injection of $A\beta_{25-35}$ were built. Morris water maze (MWM) was applied to investigate learning and memory, transmission electron microscope (TEM) to observe the ultrastructure of synapse, western blot to the proteins, electrophysiology for long-term potentiation (LTP), and Ca^{2+} concentration in synapse was also measured.

Results: The latency time in model group was significantly longer than that in sham operation group (P=0.0001); while it was significantly shorter in the OA group than that in model group (P=0.0001); compared with model group, the times of cross-platform in OA group significantly increased (P=0.0001). TEM results showed OA could alleviate neuron damage and synapses changes induced by $A\beta_{25-35}$. The expressions of CaMKII, PKC, NMDAR2B, BDNF, TrkB, and CREB protein were significantly improved by OA (P=0.0001, 0.036, 0.041, 0.0001, 0.0001, 0.026, respectively) compared with that in model group; the concentration of Ca^{2+} was significantly lower in OA group (1.11±0.42) than that in model group (1.68±0.18); and the slope rate (P=0.0001) and amplitude (P=0.0001) of f-EPSP significantly increased in OA group.

Conclusion: The present results support that OA could ameliorate Aβ-induced memory loss of AD rats by maintaining synaptic plasticity of the hippocampus.

ARTICLE HISTORY

Received: April 11, 2018
Revised: May 07, 2018
Accepted: May 22, 2018

DOI:
10.2174/1871527317666180525113109

Keywords: Alzheimer's disease, Oleanolic acid, Aβ, Ca^{2+}, long-term potentiation, synaptic plasticity.

1. INTRODUCTION

Alzheimer's disease (AD) is characterized by progressive memory loss, and the amyloid β (Aβ) peptide with its accumulation, due to overproduction and/or the failure of clearance mechanisms, followed by neuronal death, has been the upstream cause of AD over the past decades [1-3]. Abnormal Aβ accumulation and deposition in the hippocampus, the first regions of the brain to suffer damage which plays important roles in the consolidation of short-term memory, long-term memory, and spatial memory [4], is an essential process in the pathological events occurring in individuals with AD [5, 6].

Multiple studies reported that dysregulation of neuronal Ca^{2+} homeostasis also plays a pivotal role in AD pathogenesis [7, 8]. Aβ-mediated toxicity could regulate the calcium channels in the membrane to promote extracellular Ca^{2+} influx [9], and/or release intracellular Ca^{2+} pool [10, 11], to constantly enhance intracellular Ca^{2+} concentration, leading to calcium overload, which could increase the neuronal sensitivity to excitotoxicity and apoptosis [12], eventually leading to neuronal synaptic injury, resulting in learning and memory impairment. Therefore, it could improve learning and memory ability in AD patients by reducing Aβ-mediated toxicity and intracellular Ca^{2+} concentration.

*Address correspondence to this author at the Department of Neurology, the Second Hospital Affiliated to Tianjin University of Traditional Chinese Medicine, Tianjin, 300150, China; Tel/Fax: +86-22-60335418;
E-mail: zhyl220@126.com

#Kai Wang, Weiming Sun, and Linlin Zhang should be listed as co-first author.

1996-3181/18 $58.00+.00

The complicated and still unclear pathogenesis of AD made it hard to treat it. Though there are a few medications currently being used, no one has been clearly shown to delay or halt the progression of AD [13], even with many reported adverse effects [14-16], which drives researchers to look for new treatments to alter the course of AD. Nowadays, natural products and their extracts are promising drug candidates [17-19], and many of them, such as Huperzine A [20], Galantamine [21], and (-)-Epigallocatechin-3-gallate [22, 23], have shown an effect in treating AD. Similarly, many extracts from several traditional Chinese herbs such as *Astragalus membranaceus* [24], *Paeonia suffruticosa* [25], *Magnolia ofcinalis* [26], and *Rhizoma anemarrhenae* [27] have been reported to effectively prevent memory impairment.

Oleanolic acid (OA), a natural extract from the traditional Chinese herb Ligustrum lucidum (Nv Zhenzi), was found to exhibit weak anti-HIV [28], anti-HCV [29], anti-inflammatory [30, 31], and anti-cancer [32, 33] properties. Combined with other herbs, Ligustrum lucidum could delay memory loss of AD in our previous clinical study [34], and further study is still needed to investigate the mechanism of OA against the AD.

Therefore, in this study, we build AD model rats by right intracerebroventricular injection of $A\beta_{25-35}$, after intervened by OA for four weeks, to investigate whether OA could improve learning and memory deficit and its possible mechanism.

2. MATERIAL AND METHODS

2.1. Animals

Eight-week-male Sprague-Dawley rats (230-250g, from Beijing Vital River Laboratory Animal Technology Co., Ltd, Beijing, China) were kept at a 12h light/dark cycle under controlled temperature (22±2°C) and humidity (50±10%), and bred with standard diet and water ad libitum, acclimatized for 7 days before the experiments. All animal procedures were approved by the local ethical committee at Tianjin University of Traditional Chinese Medicine and met the guidelines of the Guide for the Care and Use of Laboratory Animals published by the National Institutes of Health (Documentation 55, 2001).

2.2. Drugs and Reagents

Oleanolic acid (purity>98%, Melonepharma), 2mg/mL, was suspended in 5% sodium carboxymethyl cellulose, and amyloid β-Protein Fragment 25-35 ($A\beta_{25-35}$, purity≥97%, Sigma) was dissolved in 0.9% sterile water at a concentration of 4μg/μL and incubated at 37°C for 96h to induce aggregation before usage.

The selection of OA dose in rats was calculated by equivalent dose ratio [Rat(200g):Human(70kg)=6.3], based on the clinical application of OA in patients (240mg/d/70kg), the result was 21.6mg/kg for a rat. The concentration of OA for AD rats was 2mg/mL, thus we selected the dose of 10mL/kg.

2.3. Modeling and Administration

Forty-five SD rats were randomly divided into three groups: the sham operation group, the model group, and the OA group, 15 in each group. Rats were anaesthetized by intraperitoneal injection of 10% chloral hydrate (0.3g/kg) and fixed in the rat brain stereotaxic device (Ruiwode Life Technology Co., Ltd, China). A hole was drilled on the right parietal bone (anteroposteriorly [AP], 1mm; laterally right [LR], 1.5mm; and dorsoventrally [DV], 4mm) [35]. The rats in the sham operation group received a right intracerebroventricular injection of 0.9% sterile saline 5μL (speed, 1μL/min), while the rats in the model and OA group received a right intracerebroventricular injection of $A\beta_{25-35}$ solution 5μL [36] at the same speed. The rats in OA group received OA treatments intragastricly administrated (10mL/kg) seven days after $A\beta_{25-35}$ infusion, once daily from then on before water maza test, for four weeks, while distilled water was administrated (10mL/kg) to rats in other groups.

2.4. Morris Water Maze (MWM) Test

Spatial learning ability was tested using the Morris water maze (MWM) test after four-week intragastric administration. The water maze was an open circular black tank (120cm in diameter and 60 cm in height) and a movable circular platform (8cm in diameter). A camera two meters above the tank was connected to the computer to record the rat's movement, and the data was analyzed by TopScanLite (CleverSys Inc). The tank was filled with water at a height of 23cm (23-25°C) and dyed with black edible pigment [37]. The tank was divided into 4 quadrants by two imaginary perpendicular axes with four cardinal points: North (N), South (S), East (E) and West (W), and the platform was placed in the middle of SW quadrant, 2cm submerged into the water surface.

MWM test was started with the place navigation trial, and each rat in all groups (n=15 in each group) underwent four trials per day with a one-minute-interval for 5 consecutive days. The rat was gently placed in the water from the starting position (location of SE, NE, SW, and NW quadrant, respectively), facing the wall of the tank. The rat was allowed to swim for 90 seconds until it found the submerged platform and stayed on the platform for a maximum of 10 seconds. If the rat failed to find the hidden platform within 90 seconds, it would be guided to the platform and remained on the platform for a maximum of 10 seconds before being removed from the pool. The escape latency was defined as the time taken to search for the platform within 90 seconds. The escape latency, swimming speed, and swimming path were recorded by the tracking system.

The spatial probe test was conducted 24 hours after the 5-day place navigation trial where the platform was removed from the pool to assess memory retention for the location of the platform. The rat was put into the pool at the NE point and allowed to swim for 90 seconds. The swimming speed, swimming path, and the frequency of rat crossing the virtual platform were recorded.

2.5. Transmission Electron Microscope

Rats (*n*=3 in each group) were anesthetized by intraperitoneal injection 10% chloral hydrate (0.3g/kg) after MWM test. The brain was removed rapidly and placed on ice. The CA1 region of the left hippocampus was dissected and then diced into smaller blocks of 1mm×1mm×1mm. The methods to prepare samples were as follows: the specimens were fixed by immersing in 4% buffered glutaraldehyde 4 h, and then washed in cold 1/15M phosphate buffered saline 15-30min for 3 times. The tissues were then post-fixed for 2 h in 1% osmium tetroxide, and washed in cold 1/15M phosphate buffered saline 30min for 3 times. The samples were dehydrated in ascending grades of acetone: 50%, 70%, 80%, 90%, 15 min respectively, and then in 100% acetone 15min ×2. The tissues were infiltrated in embedding medium for 3 h at room temperature, 60 min in mixture of 100% acetone/embedding medium (1:1) in 37°C, overnight in mixture of 100% acetone/embedding medium (1:3) in 37°C, 5 h in embedding medium in 37°C. All tissues were embedded and then cured in a 37°C oven for 24 h followed by 48 h in a 60°C oven. The samples were sliced into 50nm with an ultramicrotome (Leica UCT, Germany). The samples were stained with uranyl acetate for 45 min, and then stained with lead citrate for 15 min. A transmission electron microscope (TEM) (Hitachi H7500, Japan) was used to observe the neurons using.

2.6. Western Blot Analysis

Rats (*n*=5 in each group) were sacrificed for extracting protein samples from right hippocampi after MWM test by splitting, centrifugation, and boiling. Equal amounts (40 μg) of protein were loaded into each well of a sodium dodecyl sulfate-polyacrylamide gel (10% polyacrylamide gels) and separated by electrophoresis. The proteins were then transferred to nitrocellulose membranes (Amersham, USA), which were blocked with 5 % bovine serum albumin and prepared in a Tris-buffered saline (TBS) overnight at 4°C. The membranes were incubated with antibodies to detect CaMKⅡ (ab134041, 1:1000), PKC (ab136491, 1:1000), NMDAR2B (ab65783, 1:1000), BDNF (ab205067, 1:1000), TrkB (sc-377218, 1:1000), CREB (ab32515, 1:1000), GAPDH (ab8245, 1:1000) and beta Actin (ab184220 1:1000), followed by incubation with appropriate HRP-conjugated goat anti-rabbit (ZSGB-BIO, China; ZB-5301, 1:1,000) or HRP-conjugated goat anti-mouse secondary antibodies (ZSGB-BIO, China; ZB-5305, 1:1,000). Immunoreactive bands were visualized using the BeyoECL Plus (Beyotime Company, China), and the resulting membranes were imaged using the VersaDoc MP5000 imaging system (BIO-RAD, USA). The Quantity One was used to assess the band intensity and to carry out semi-quantitative analyses.

2.7. Measurement of Ca^{2+} Concentration

Rats (*n*=3 in each group) were intraperitoneally injected with 10% chloral hydrate (0.3g/kg) after the MWM tests, and the right hippocampi were rapidly separated. They were weighed and homogenized in an isotonic sucrose solution (0.32 mol/L) at 4°C in 1 g: 10 mL. The homogenate was centrifuged at 500g for 10 min to get the supernatant and then centrifuged at 4°C for 20 min (10000 g) to obtain the crude synaptosomal. The crude synaptosome was suspended with 0.32 mol/L sucrose solution, and then carefully spread over the density gradient of 0.8M and 1.2M sucrose. They were centrifuged with high-speed at 50000 g for 25 min to obtain the synaptosomes, and centrifuged at 2000 g for in 4°C to take precipitation [38]. The synaptosomes were quantified by BCA method and equal amounts (30 μg) of synaptosomes were added to each well of the black 96-well cell culture plate. Rhod 2-AM (1:500) probe 100 μL was added and incubated at 37°C for 30 min away from light. The culture medium was placed in a fluorescent microplate reader (BioTek FLx800, USA) to measure the fluorescence intensity at excitation wavelength of 557 nm and emission wavelength of 581 nm. Formula: $[Ca^{2+}]i=K_d(F-F_{min})/(F_{max}-F)$.

2.8. Electrophysiology

After the MWM test, long-term potentiation was quantified with *in vivo* electrophysiological techniques. Rats (*n*=3in each group) were anaesthetized with an intraperitoneal injection of 20% urethane (1.2 g/kg), and then were positioned in a stereotaxic apparatus (Narishige, Japan) for surgery, covered with a towel to keep warm. A 3cm incision, blunt off the skin periosteum was cut to fully expose the bregma, sagittal suture, and parietal. A hole in the skull was drilled to expose CA3 region (4.2mm posterior to the bregma, 3.8mm right to the sagittal suture, 2.0 mm-3.5mm beneath the cortex) and CA1 region (3.4 mm posterior to the bregma, 2.5mm right to the sagittal suture, 1.5 mm-2.5mm beneath the cortex), coordinated according to the mouse brain atlas [35]. A bipolar stimulation electrode was placed in the CA3 region and a monopolar stainless steel recording electrode in the CA1 region. Stimulus-response was tested using a range of stimulation intensities from 0.1mA to 1 mA with 0.2ms，0.03HZ to determine the appropriate stimulating. The stimulating intensity (range 0.3-0.5 mA, stimulus pulse with 0.2 ms, at 0.03 Hz) that could evoke a response of 70% of its maximum amplitude was chosen for the following experiment.

The basal field excitatory postsynaptic potentials (fEPSP) were recorded for 20 min with a single pulse of 2 times every minute. LTP was evoked by theta burst stimulation (TBS): 10 trains at 5 Hz consisting of 10 single pulses at 100 Hz. The f-EPSP was recorded for 60 min with a single pulse of 1 time every minute. LTP analysis was carried out in ClampFit (Molecular Devices, USA) and figures were constructed in KaleidaGraph (Synergy Sofware, Reading, PA, USA) using values for the amplitude of the fEPSP.

2.9. Statistical Analysis

Statistical analysis was performed with the Statistical Package for the Social Sciences (SPSS) v19.0, and all data were presented as Mean±SD. For the repeated measurement data (speed and escape latency time), repeated measurement analysis of variance (ANOVA) was applied to speed, and taking the sample size and normality, Generalized Estimating Equations analysis was applied to escape latency time; for other results, one way analysis of variance was applied with post-hoc LSD to data according to normality and homogeneity variance; or nonparametric test with Kruskal-Wallis was applied. The threshold for significance was set at $P<0.05$ for all analyses.

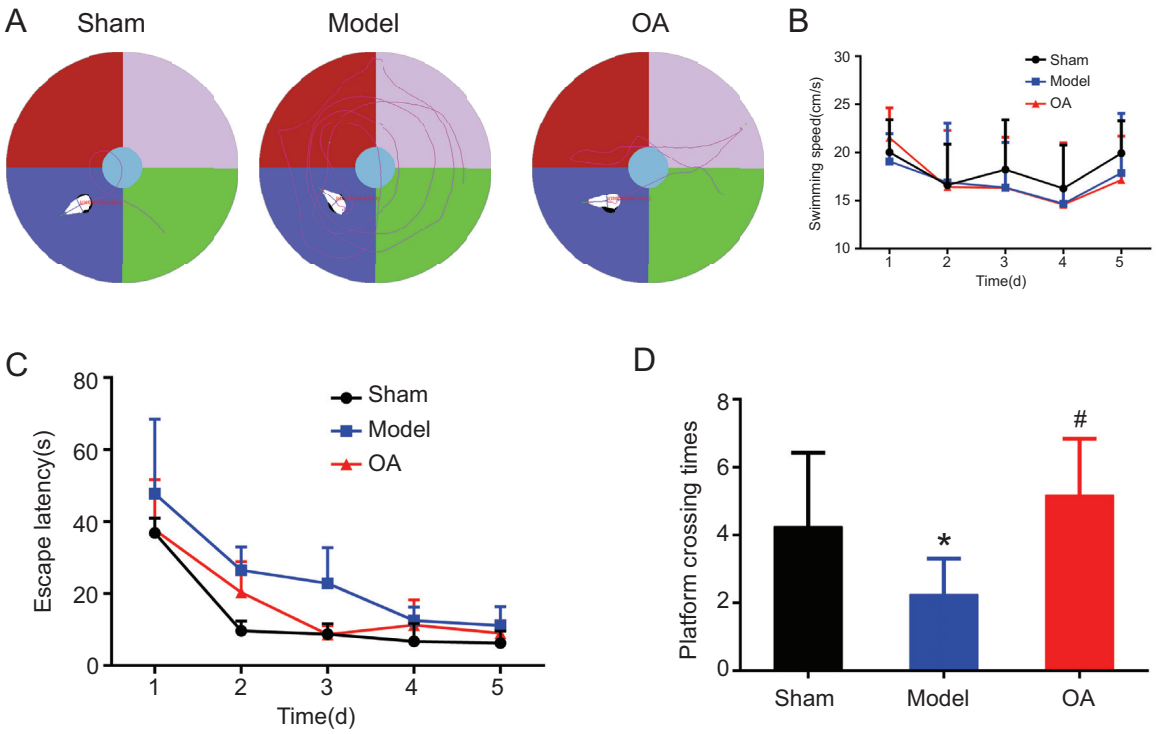

Fig. (1). Results of Morris water maze test(n=15). (**A**) Swimming paths of rats in each group in the Morris water maze. (**B**) Average swimming speed of rats in each group. Repeated measurement ANOVA results showed that there was no significant difference of the average swimming speed in each group (F=0.331, P = 0.721>0.05) (**C**) Escape latency time of rats in each group. Post Pairwise Comparisons using Bonferroni method showed that the latency time in model group was significantly longer than that in sham operation group (P=0.0001<0.05); while it was significantly shorter in the OA group than that in model group (P=0.0001<0.05) (**D**) platform crossing times of rats in each group. Post comparison with LSD method showed that compared with sham group, the times of cross-platform in model group significantly decreased (P = 0.007 <0.05); while compared with model group, the times of cross-platform in OA group significantly increased (P = 0.0001 <0.05).
Notes: *indicates compared with that in the sham operation group, P<0.05;
#indicates compared with that in the model group, P<0.05.

3. RESULTS

3.1. OA Improves Spatial Learning and Memory Performance in the MWM Test

Swimming paths of rats in each group in the MWM test are presented in Fig. (**1A**). Repeated measurement ANOVA results showed that there was no significant difference in the average swimming speed in each group (F=0.331, P=0.721>0.05) (Fig. **1B**).

3.1.1. Escape Latency

In the MWM test, the escape latency was gradually shortened during the training period. Based on the Generalized Estimating Equations analysis, there was significant difference among three groups (P = 0.002<0.05), but no interaction between groups and time (P = 0.063> 0.05) (Table **1**). Based on the Estimated Marginal Means, the escape latency showed sham operation group < OA group < model group (Table **2**). Post Pairwise Comparisons using Bonferroni method showed that the latency time in model group was significantly longer than that in sham operation group (P=0.0001<0.05); while it was significantly shorter in the OA group than that in model group (P=0.0001<0.05).

Table 1. Tests model effects.

-	Wald Chi-square Value	Variance	Sig.
(Intercept)	333.317	1	0.0001
Groups	12.827	2	0.002
Time	190.298	1	0.0001
Groups×Times	5.523	2	0.063

Table 2. Estimated marginal means of escape latency.

Groups	Mean	Standard Error	95% Wald Confidence Interval	
			Lower	Upper
Sham	13.95	2.03	9.97	17.94
Model	24.64	2.11	20.51	28.78
OA	16.89	2.29	12.40	21.37

3.1.2. Spatial Probe Test

One-way ANOVA analysis showed that there was a statistically significant difference among three groups ($F = 9.056$, $P = 0.001 < 0.05$). Post comparison with LSD method showed that compared with sham group, the times of cross-platform in model group significantly decreased ($P = 0.007 < 0.05$); while compared with model group, the times of cross-platform in OA group significantly increased ($P = 0.0001 < 0.05$) (Fig. **1D**).

3.2. OA Alleviates Neuron Damage and Synapses Changes Induced by $A\beta_{25-35}$

TEM revealed that in the sham operation group, the neurons were intact, with homogeneous nuclei, abundant organelles, oval and full mitochondria, clear and intact double layer structure of the cristal membrane, endoplasmic reticulum attached with a large number of ribosomes. The synapses were normal with abundant synaptic vesicles secreted by presynaptic elements. The synaptic cleft was narrow, and the postsynaptic density was centralized (Fig. **2A-C**).

In the model group, neurons were not intact, with shrinking nuclei, severe disruption of organelles, rarely normal mitochondria in vacuolar state, ruptured endoplasmic reticulum with obvious loss of ribose. The abundance of synaptic vesicles secreted by presynaptic elements decreased. The synaptic cleft clearly widened, with sparse postsynaptic density (Fig. **2D-F**).

In the OA group, structures of neurons were intact on the whole, with homogeneous nuclei, abundant organelles, slightly swollen mitochondria, partial fusion and fracture of cristal membrane, slight loss of ribose of endoplasmic reticulum. Abundant synaptic vesicles secreted by presynaptic elements could be observed. The synaptic cleft was clear, without obvious widening, and the postsynaptic density was centralized (Fig. **2G-I**).

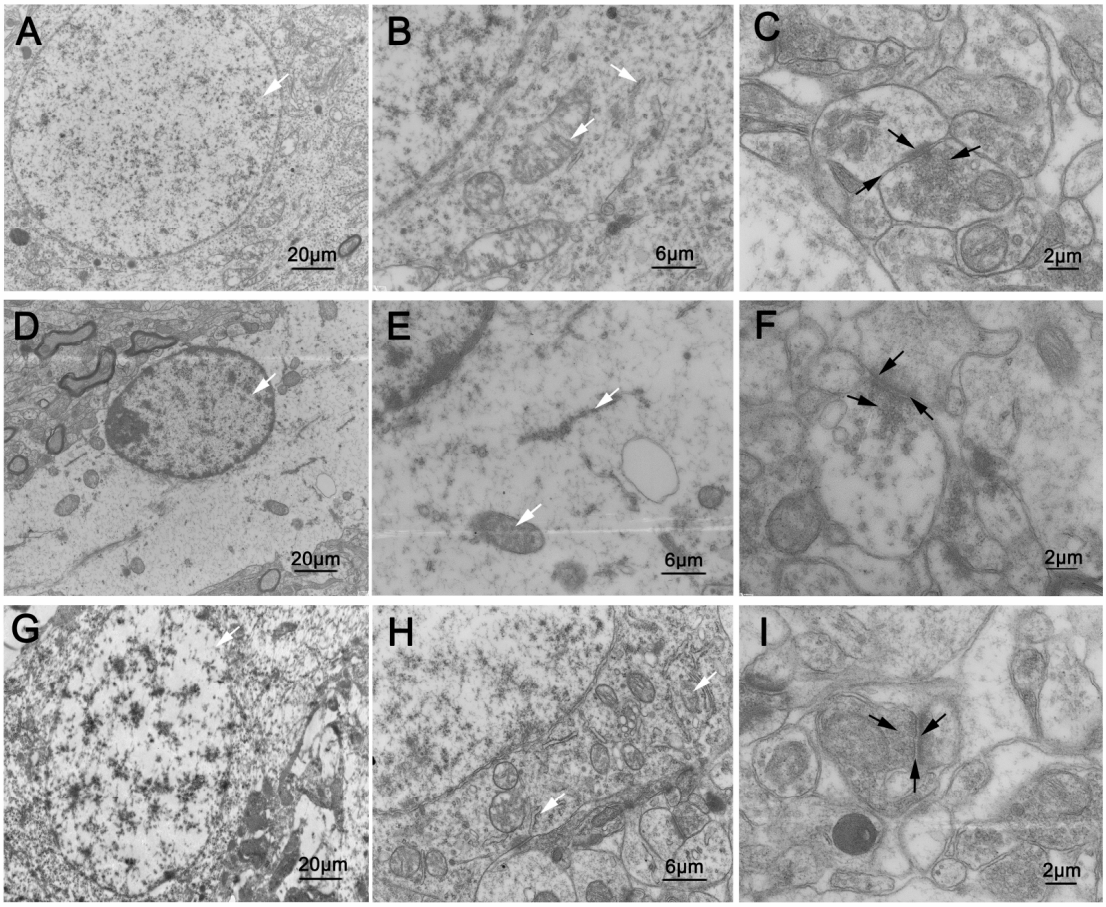

Fig. (2). Ultrastructure of neurons and synapses (n=3). In the sham operation group: (**A**, **B**) the neurons were intact, with homogeneous nuclei, abundant organelles, oval and full mitochondria, clear and intact double layer structure of the cristal membrane, endoplasmic reticulum attached with a large number of ribosomes (white arrows). (**C**) the synapses were normal with many synaptic vesicles secreted by presynaptic elements. The synaptic cleft was narrow, and the postsynaptic density was centralized (black arrows). In the model group: (**D**, E) neurons were not intact, with shrinking nuclei, severe loss of organelles, rarely normal mitochondria in vacuolar state, ruptured endoplasmic reticulum with obvious loss of ribose (white arrows). (**F**) the amount of synaptic vesicles secreted by presynaptic elements decreased. The synaptic cleft clearly widened, with sparse postsynaptic density (black arrows). In the OA group: (**G**, **H**) structures of neurons were intact on the whole, with homogeneous nuclei, abundant organelles, slightly swollen mitochondria, partial fusion and fracture of cristal membrane, slight loss of ribose of endoplasmic reticulum (white arrows). (**I**) abundant synaptic vesicles secreted by presynaptic elements could be observed. The synaptic cleft was clear, without obvious widening, and the postsynaptic density was centralized (black arrows).

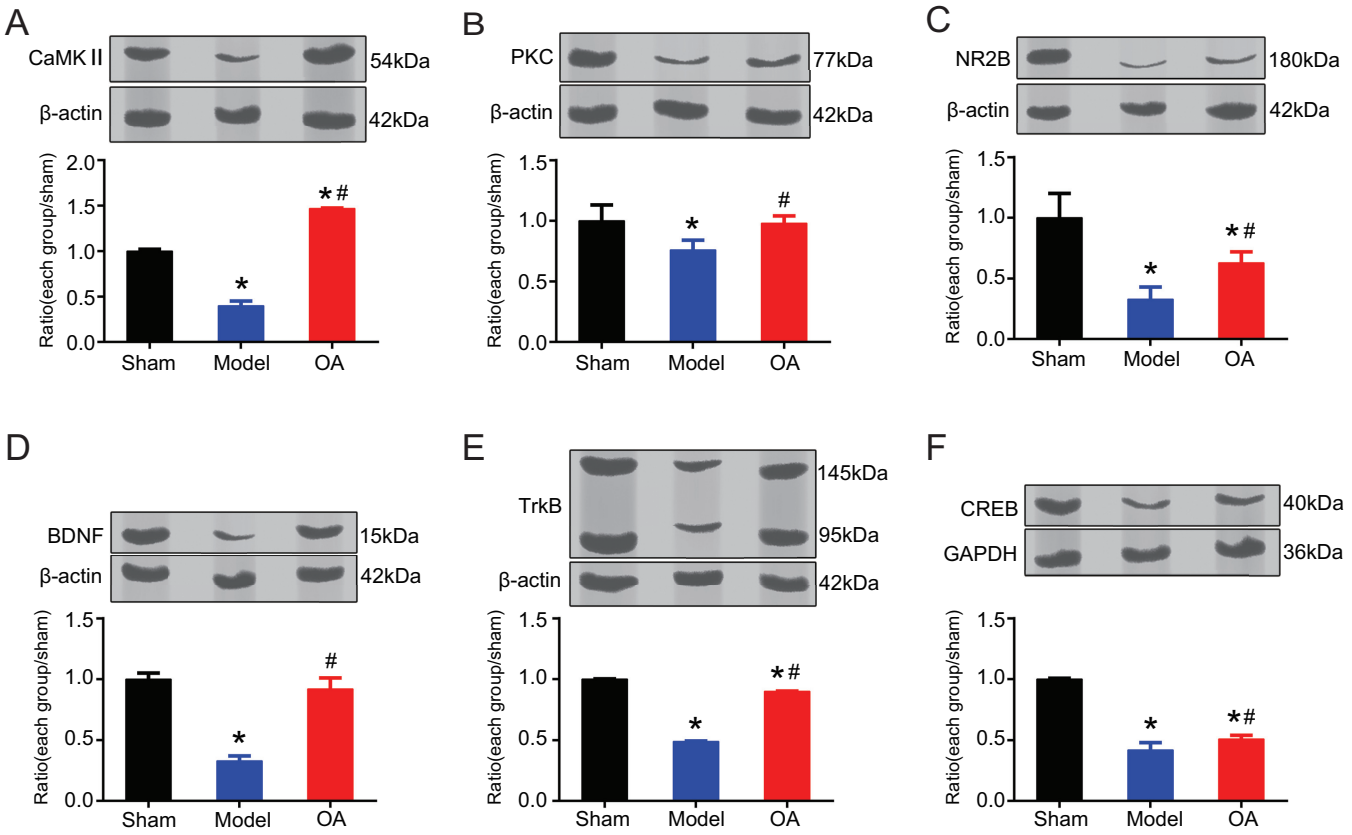

Fig. (3). Expression of CaMKII, PKC, NMDAR2B, BDNF, TrkB, and CREB protein (cropped blots from different gels). (**A**) Compared with that in the sham operation group, the expression of CaMKII was significantly lower in the model group (P=0.0001). While compared with that in the model group, the expression of CaMKII was significantly higher in the OA group (P=0.0001), and higher than that in sham group (P=0.0001); (**B**) compared with that in the sham operation group, the expression of PKC was significantly lower in the model group (P=0.026). While compared with that in the model group, the expression of PKC was significantly higher in the OA group (P=0.036); (**C**) compared with that in the sham operation group, the expression of NMDAR2B was significantly lower in the model group (P=0.001). While compared with that in the model group, the expression of NMDAR2B was significantly higher in the OA group (P=0.041), but still significantly lower than that in sham group (P=0.018); (**D**) compared with that in the sham operation group, the expression of BDNF was significantly lower in the model group (P=0.0001). While compared with that in the model group, the expression of BDNF was significantly higher in the OA group (P=0.0001); (**E**) compared with that in the sham operation group, the expression of TrkB was significantly lower in the model group (P=0.0001). While compared with that in the model group, the expression of TrkB was significantly higher in the OA group (P=0.0001), but still significantly lower than that in sham group (P=0.0001); (**F**) compared with that in the sham operation group, the expression of CREB was significantly lower in the model group, with statistically significant difference (P=0.0001). While compared with that in the model group, the expression of CREB was significantly higher in the OA group, with statistically significant difference (P=0.0001), but still significantly lower than that in sham group (P=0.0001).

Notes:*indicates compared with that in the sham operation group, P<0.05.

#indicates compared with that in the model group, P<0.05.

3.3. OA could Improve the Expression of CaMKII, PKC, NMDAR2B, BDNF, TrkB, and CREB Protein

We measured protein levels of CaMKII, PKC, NMDAR2B, BDNF, TrkB, and CREB of the three groups. One way ANOVA results showed that there existed inter-group difference (CaMKII, F=1054.102, P=0.0001<0.05; PKC, F=5.346, P=0.046<0.05; NMDAR2B, F=16.949, P=0.003<0.05; BDNF, F=95.467, P=0.0001<0.05; TrkB, F=40049.417, P=0.0001<0.05, CREB, F=196.703, P=0.0001 <0.05). Post hoc statistics using LSD showed that compared with that in the sham operation group, the expression of CaMKII (Fig. **3A**), PKC (Fig. **3B**), NMDAR2B (Fig. **3C**), BDNF (Fig. **3D**), TrkB (Fig. **3E**), and CREB (Fig. **3F**) were significantly lower in the model group, with statistically significant difference (P=0.0001, 0.026, 0.001, 0.0001, 0.0001, 0.0001, respectively). While compared with that in the model group, the expression of CaMKII (Fig. **3A**), PKC (Fig. **3B**), NMDAR2B (Fig. **3C**), BDNF (Fig. **3D**), TrkB (Fig. **3E**), and CREB (Fig. **3F**) were significantly higher in the OA group, with statistically significant difference (P=0.0001, 0.036, 0.041, 0.0001, 0.0001, 0.026, respectively). The levels of NR2B, Trkb, and CREB in OA group were still significantly lower than that in sham group (P=0.018<0.05, P=0.000 <0.05, P=0.000<0.05, respectively). The levels of BDNF and

PKC in OA group were lower than that in sham group, but the difference was not statistically significant (P=0.165> 0.05, P=0.808>0.05, respectively). The level of CAMKII in OA group was higher than sham group, with significant difference (P=0.000<0.05).

3.4. OA Could Decrease the Concentration of Ca^{2+}

Kruskal-Wallis test showed that compared with that in the sham operation group, the concentration of Ca^{2+} was significantly higher in the model group, with statistically significant difference (P=0.0001). While compared with that in the model group, the concentration of Ca^{2+} was significantly lower in the OA group, with statistically significant difference (P=0.015) (Table **3**).

Table 3. Ca^{2+} concentration of each group (Mean±SD).

Group	n	Rhod-2 Fluorescence
Sham operation	3	0.96±0.09
Model	3	1.68±0.18*
OA	3	1.11±0.42#

Notes: *indicates compared with that in the sham operation group, P<0.05.
#indicates compared with that in the model group, P<0.05

3.5. OA Could Increase the Slope and Amplitude of f-EPSP

In the LTP assay, the stimulation electrode (SE) was placed in the CA3 region and the recording electrode (RE) in the CA1 region (Fig. **4A**). Following the TBS stimulation (Fig. **4B**), the fEPSPs slopes were recorded. Kruskal-Wallis test showed that the slope rate significantly decreased after high frequency stimulation in the model group compared with that in the sham operation group (P=0.0001). While compared with model group, the slope rate significantly increased after high frequency stimulation in the OA group (P=0.0001) (Fig. **4C**).

Kruskal-Wallis test showed that the amplitude significantly decreased after high frequency stimulation in the model group compared with that in the sham operation group (P=0.0001). While compared with model group, the amplitude significantly increased after high frequency stimulation in the OA group (P=0.0001) (Fig. **4D**).

4. DISCUSSION

AD is the most common form of dementia in the elderly, and it is characterized clinically by progressive cognitive impairment, memory loss, and altered behavior [39-41]. Several hypotheses have been proposed, and it is widely accepted that Aβ plays a central role [42, 43]. In our study, we

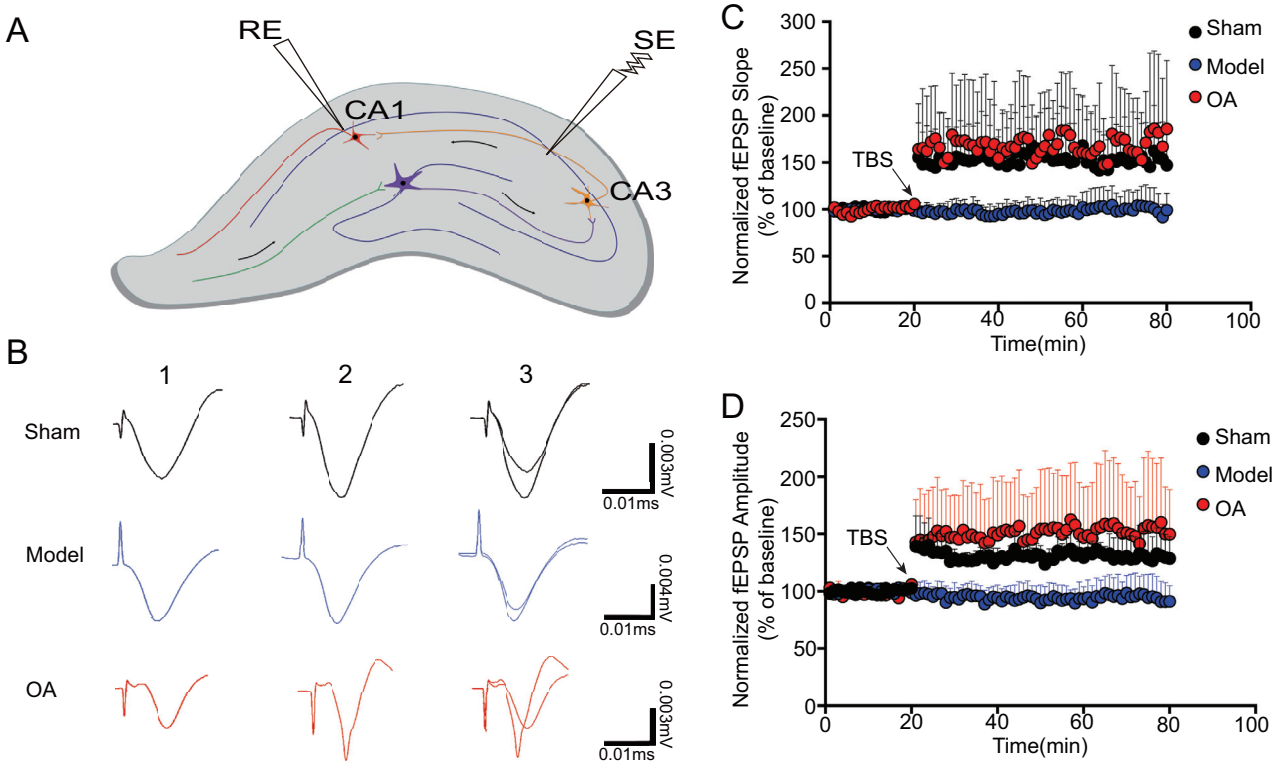

Fig. (4). OA rescues Aβ-induced deficits in long-term potentiation (n=3). (**A**) Position of stimulation electrode (SE) and recording electrode (RE); (**B**) 1: potential of resting state; 2: 60 min after TBS; 3: combination of (1) and (2) in each group; (**C**) slope change in each group. Kruskal-Wallis test showed that the slope rate significantly decreased after high frequency stimulation in the model group compared with that in the sham operation group (P = 0.0001). While compared with model group, the amplitude significantly increased after high frequency stimulation in the OA group (P=0.0001) (**D**) amplitude change in each group. Kruskal-Wallis test showed that the amplitude significantly decreased after high frequency stimulation in the model group compared with that in the sham operation group (P=0.0001). While compared with model group, the amplitude significantly increased after high frequency stimulation in the OA group (P=0.0001)

build the AD model by injecting $A\beta_{25-35}$ aggregate into right ventricle, which is a widely used model to study AD [44, 45]. It has been reported that Aβ injection would cause memory impairment [46, 47], and the results in our study that the escape latency increased and the frequency of platform crossing decreased in MWM test of rats in model group also proved that. While the lower escape latency and higher frequency of platform crossing in OA group represent that OA could ameliorate Aβ-induced spatial learning and memory loss of AD rats.

It is widely accepted that the synapses play an important role in the formation of memory [48-50]. In the nervous system, synapses are esseential to neuronal functions:a synapse is a structure where a neuron could pass an electrical or chemical signal to another neuron. Evidences show that synapse loss or synaptic dysfunction is strongly correlated with memory impairment in AD, suggesting a causal role for dwindling synaptic integrity in the etiology of AD [51, 52]. Synapse is formed by presynaptic axon ending and by postsynaptic dendritic spine, and a similar loss of both presynaptic and post-synaptic components [53] as well as significant decreases in synaptic density of the hippocampus could occur in AD brains [54-56]. Synapse loss, suppressed presynaptic vesicle release [57, 58], and changes in the shape and size of dendritic spines [59] caused by Aβ deposition are the pathological hallmarks of AD, which was also found in our rats of model group by TEM. Our research showed that OA exhibited a positive effect on preserving neuron injury, improving the arrangements and the ultrastructure of neurons, and maintaining synaptic integrity, which suggested a protection and improvement of memory of AD rats.

Change in pre-synaptic and post-synaptic components by a high local concentration of Aβ oligomers could affect neuronal Ca^{2+} homeostasis [60], which is a popular hypothesis of AD in recent years [61, 62]. The imbalance of Ca^{2+} homeostasis leading to extracellular Ca^{2+} flow into the cytoplasm, could cause Ca^{2+} overload. A persistent elevation of Ca^{2+} concentration could not only constantly disrupt memories but also contribute to neuronal cell death. Furthermore, it actually occurs prior to cognitive decline and extensive neuronal death in AD [63]. In our study, the injection of $A\beta_{25-35}$ led to synaptic Ca^{2+} overload in model group, then causing neurotoxicity; while OA could effectively reduce synaptic Ca^{2+} concentration, and exhibited the role of neuroprotection to improve learning and memory deficit.

Meanwhile, both pre-synaptic and post-synaptic mechanisms can contribute to the expression of synaptic plasticity, one of the important neurochemical foundations of learning and memory [64, 65]. Presynaptic vesicle could release neurotransmitters which are directly proportional to synaptic transmission strength. There are a lot of proteins such as N-methyl-Daspartate receptor (NMDARs), calmodulin-dependent-protein kinase II (CaMKII), and protein kinase C (PKC) in postsynaptic density (PSD), and the destruction of PSD could inactivate synaptic proteins, influence synaptic homeostasis, leading to negative synaptic formation and synaptic loss and dysfunction in AD [66, 67]. NMDAR, CaMKII, and PKC in PSD play essential roles in synaptic plasticity. The accumulated evidences demonstrated NMDAR was dysfunctional, and the protein activation of CaMKII and PKC was suppressed in AD. In our study, NMDAR2B, CaMKII and PKC protein expression, all significantly decreased in model group. We also found that OA could increase the NMDAR2B, CaMKII and PKC protein expression, to restore and maintain synaptic plasticity.

Long-term potentiation (LTP), a main form of long-term synaptic plasticity, is an increase in synaptic response following potentiating pulses of electrical stimuli, and the induction and maintenance of it could reflect the strength of synaptic transmission efficiency, which was widely considered as one of the major cellular mechanisms underlying learning and memory [68-70]. It has been reported that LTP of hippocampal CA1 area was significantly inhibited in $A\beta_{25-35}$ induced learning-and-memory-impairment rats [71]. Moreover, when the way to form LTP was blocked, learning and memory would be inhibited, suggesting that the cognitive decline in individuals with AD might result from impaired LTP [72, 73]. In our study, the slope and amplitude of fEPSP were taken as reference values for LTP (fEPSP to reflect the amount of excitatory synapse, slope to reflect the speed of synaptic response to stimuli, and amplitude to the intensity of synaptic stimulation). Before TBS, the amplitude and slope of fEPSP in the model group and sham operation group were consistent; while after TBS, the amplitude and slope of fEPSP in the model group were significantly lower than those in the sham operation group, suggesting that $A\beta_{25-35}$ does not affect the basic function of synaptic transmission, but it inhibits TBS induced LTP. Our results also showed that OA could increase the amplitude and slope of fEPSP in AD models, indicating it could enhance the synaptic transmission.

In the maintenance and induction of LTP, brain-derived neurotrophic factor (BDNF), as a major regulator of synaptic structure and function, through tyrosine kinase B (TrkB) plays an essential role [74, 75], and reduced BDNF/TrkB leads to impaired spatial memory in AD. The increased BDNF/TrkB expression could activate Cyclic AMP response element binding protein (CREB), a constitutively expressed nuclear transcription factor that regulates the expression of genes involved in cognition and neuronal survival [76]. CREB shows a well-documented role in the formation and retention of memory by mediating gene expression in the hippocampus during LTP [77, 78]. CREB down-regulation is implicated in AD and increasing the expression of CREB is being considered as a possible therapeutic target for AD [79]. In our study, the expression of BDNF, TrkB, CREB proteins were all significantly suppressed in model group, while OA showed an up-regulating effect on them to enhance LTP.

CONCLUSION

In conclusions, we found that OA could ameliorate Aβ-induced memory loss of AD rats, which has never been reported before. And during the treatment, OA showed a protective effect in maintaining synaptic integrity to restore synaptic plasticity by increasing the NMDAR2B, CaMKII and PKC protein expression in PSD, reducing synaptic Ca^{2+} concentration, enhancing the inhibited LTP after $A\beta_{25-35}$ injection by up-regulating the expression of BDNF, TrkB, CREB proteins, which might be its mechanism in improving learning and memory deficit.

LIST OF ABBREVIATIONS

AD	=	Alzheimer's Disease
Aβ	=	Amyloid β
OA	=	Oleanolic Acid
MWM	=	Morris Water Maze
fEPSP	=	Field Excitatory Postsynaptic Potentials
TBS	=	Theta Burst Stimulation

ETHICS APPROVAL AND CONSENT TO PARTICIPATE

All animal procedures were approved by the local ethical committee at Tianjin University of Traditional Chinese Medicine.

HUMAN AND ANIMAL RIGHTS

No human were used in this study the guidelines for animals were guided from the Care and Use of Laboratory Animals published by the National Institutes of Health (Documentation 55, 2001).

CONSENT FOR PUBLICATION

Not applicable.

CONFLICT OF INTEREST

The authors declare no conflict of interest, financial or otherwise.

ACKNOWLEDGEMENTS

Kai Wang, Weiming Sun, Wei Guo, Linlin Zhang,and Jiachun Xu made substantial contributions to conception, design, and performing of the experiment. Shuang Liu, Zhen Zhou, and Yulian Zhang analyze the data and are involved in drafting the manuscript. All authors read and approved the final manuscript.

This work is supported by National Natural Science Foundation of China (grant numbers: 81473490, 81273940), and Science and Technology Program of Tianin (grant number: 15ZXLCSY00020).

We acknowledge the contributions by Yang Cao, Congcong Bi, Yifu Wang, Xueyan Wang, Yan Ma, Hui Qin, Qijing Qin during the work. We would like to thank the Department of Electron Microscopy Center Hebei Medical University for our work, and we would be grateful to all the teachers for their help in making EM sample, and taking EM images.

REFERENCES

[1] Leissring MA. Abeta-Degrading proteases: Therapeutic potential in alzheimer disease. CNS Drugs 2016; 30(8): 667-75.

[2] Fyfe I. Alzheimer disease: Anti-Abeta antibody treatment shows promise in Alzheimer disease. Nat Rev Neurol 2016; 12(10): 554-5.

[3] Yamamoto K, Tanei Z, Hashimoto T, *et al.* Chronic optogenetic activation augments abeta pathology in a mouse model of Alzheimer disease. Cell Rep 2015; 11(6): 859-65.

[4] Eichenbaum H. The hippocampus and declarative memory: cognitive mechanisms and neural codes. Behav Brain Res 2001; 127(1-2): 199-207.

[5] Mancini S, Minniti S, Gregori M, *et al.* The hunt for brain Abeta oligomers by peripherally circulating multi-functional nanoparticles: Potential therapeutic approach for Alzheimer disease. Nanomedicine 2016; 12(1): 43-52.

[6] Meisl G, Yang X, Frohm B, *et al.* Quantitative analysis of intrinsic and extrinsic factors in the aggregation mechanism of Alzheimer-associated Abeta-peptide. Sci Rep 2016; 6: 18728.

[7] Berridge MJ. Dysregulation of neural calcium signaling in Alzheimer disease, bipolar disorder and schizophrenia. Prion 2013; 7(1): 2-13.

[8] Daschil N, Kniewallner KM, Obermair GJ, *et al.* L-type calcium channel blockers and substance P induce angiogenesis of cortical vessels associated with beta-amyloid plaques in an Alzheimer mouse model. Neurobiol Aging 2015; 36(3): 1333-41.

[9] Rovira C, Arbez N, Mariani J. Abeta(25-35) and Abeta(1-40) act on different calcium channels in CA1 hippocampal neurons. Biochem Biophys Res Commun 2002; 296(5): 1317-21.

[10] Ferreiro E, Oliveira CR, Pereira C. Involvement of endoplasmic reticulum Ca2+ release through ryanodine and inositol 1, 4, 5-triphosphate receptors in the neurotoxic effects induced by the amyloid-beta peptide. J Neurosci Res 2004; 76(6): 872-80.

[11] Lopez JR, Lyckman A, Oddo S, *et al.* Increased intraneuronal resting [Ca2+] in adult Alzheimer's disease mice. J Neurochem 2008; 105(1): 262-71.

[12] Mattson MP. Pathways towards and away from Alzheimer's disease. Nature 2004; 430(7000): 631-9.

[13] Birks JS, Grimley Evans J. Rivastigmine for Alzheimer's disease. Cochrane Database Syst Rev 2015(4): CD001191.

[14] Dysken MW, Sano M, Asthana S, *et al.* Effect of vitamin E and memantine on functional decline in Alzheimer disease: The TEAM-AD VA cooperative randomized trial. JAMA 2014; 311(1): 33-44.

[15] Murgai AA, LeDoux MS. Memantine-induced Myoclonus in a Patient with Alzheimer Disease. Tremor Other Hyperkinet Mov (N Y) 2015; 5: 337.

[16] Pilotto A, Franceschi M, D'Onofrio G, *et al.* Effect of a CYP2D6 polymorphism on the efficacy of donepezil in patients with Alzheimer disease. Neurology 2009, 73(10): 761-7.

[17] Dey A, Bhattacharya R, Mukherjee A, *et al.* Natural products against Alzheimer's disease: Pharmaco-therapeutics and biotechnological interventions. Biotechnol Adv 2017; 35(2): 178-216.

[18] Wei S. Potential therapeutic action of natural products from traditional Chinese medicine on Alzheimer's disease animal models targeting neurotrophic factors. Fundam Clin Pharmacol 2016; 30(6): 490-501.

[19] Hielscher-Michael S, Griehl C, Buchholz M, *et al.* Natural products from Microalgae with potential against Alzheimer's Disease: Sulfolipids are potent Glutaminyl Cyclase Inhibitors. Mar Drugs 2016; 14(11): 203.

[20] Damar U, Gersner R, Johnstone JT, *et al.* Huperzine A: A promising anticonvulsant, disease modifying, and memory enhancing treatment option in Alzheimer's disease. Medical Hypotheses 2017; 99: 57-62.

[21] Nakagawa R, Ohnishi T, Kobayashi H, *et al.* Long-term effect of galantamine on cognitive function in patients with Alzheimer's disease versus a simulated disease trajectory: An observational study in the clinical setting. Neuropsy Dis Treat 2017; 13: 1115-24.

[22] Chang X, Rong CP, Chen YB, *et al.* (-)-Epigallocatechin-3-gallate attenuates cognitive deterioration in Alzheimer's disease model mice by upregulating neprilysin expression. Experimental Cell Research 2015; 334(1): 136-45.

[23] Dragicevic N, Smith A, Lin X, *et al.* Green Tea Epigallocatechin-3-Gallate (EGCG) and other flavonoids reduce Alzheimer's Amyloid-Induced Mitochondrial Dysfunction. J Alzheimers Dis 2011; 26(3): 507-21.

[24] Li WZ, Wu WY, Huang DK, *et al.* Protective effects of astragalosides on dexamethasone and Aβ25-35 induced learning and memory impairments due to decrease amyloid precursor protein expression in 12-month male rats. Food & Chemical Toxicology

An International Journal Published for the British Industrial Biological Research Association, 2012, 50(6): 1883-90.

[25] Su SY, Cheng CY, Tsai TH, *et al.* Paeonol Protects Memory after Ischemic Stroke via Inhibiting β-Secretase and Apoptosis. Evidence-based complementary and alternative medicine : eCAM, 2011; 2012(10): 932823.

[26] Lee YJ, Choi DY, Sang BH, *et al.* Inhibitory effect of ethanol extract of magnolia officinalis on memory impairment and amyloidogenesis in a transgenic mouse model of alzheimer's disease via regulating β-secretase activity. Phytotherapy Research 2012; 26(12): 1884-92.

[27] Huang JF, Lei S, Pei L, *et al.* Timosaponin-BII inhibits the up-regulation of BACE1 induced by Ferric Chloride in rat retina. BMC Complementary and Alternative Medicine 2012; 12(1): 189.

[28] Mengoni F, Lichtner M, Battinelli L, *et al. In vitro* anti-HIV activity of oleanolic acid on infected human mononuclear cells. Planta Med 2002; 68(2): 111-4.

[29] Ma CM, Wu XH, Masao H, *et al.* HCV protease inhibitory, cytotoxic and apoptosis-inducing effects of oleanolic acid derivatives. J Pharm Pharm Sci 2009; 12(3): 243-8.

[30] Bednarczyk-Cwynar B, Wachowiak N, Szulc M, *et al.* Strong and long-lasting antinociceptive and anti-inflammatory conjugate of naturally occurring oleanolic acid and aspirin. Front Pharmacol 2016, 7: 202.

[31] Kashyap D, Sharma A, Tuli HS, *et al.* Ursolic Acid and Oleanolic Acid: Pentacyclic Terpenoids with promising anti-inflammatory activities. Recent Pat Inflamm Allergy Drug Discov 2016; 10(1): 21-33.

[32] Amara S, Zheng M, Tiriveedhi V. Oleanolic Acid inhibits high salt-induced exaggeration of warburg-like metabolism in breast cancer cells. Cell Biochem Biophys 2016; 74(3): 427-34.

[33] Mu DW, Guo HQ, Zhou GB, *et al.* Oleanolic acid suppresses the proliferation of human bladder cancer by Akt/mTOR/S6K and ERK1/2 signaling. Int J Clin Exp Pathol 2015; 8(11): 13864-70.

[34] Zhang Y, Lin C, Zhang L, *et al.* Cognitive improvement during treatment for mild alzheimer's disease with a chinese herbal formula: A randomized controlled trial. PLoS One 2015; 10(6): e0130353.

[35] Paxinos G, Watson C. The Rat Brain in Stereotaxic Coordinates - The New Coronal Set, Fifth Edition2004.

[36] Galoyan AA, Sarkissian JS, Chavushyan VA, *et al.* Neuroprotection by hypothalamic peptide proline-rich peptide-1 in Abeta25-35 model of Alzheimer's disease. Alzheimers Dement 2008; 4(5): 332-44.

[37] Vorhees CV, Williams MT. Morris water maze: Procedures for assessing spatial and related forms of learning and memory. Nat Protoc 2006; 1(2): 848-58.

[38] Gray EG, Whittaker VP. The isolation of nerve endings from brain: An electron-microscopic study of cell fragments derived by homogenization and centrifugation. J Anat 1962; 96: 79-88.

[39] Brookmeyer R, Kawas CH, Abdallah N, *et al.* Impact of interventions to reduce Alzheimer's disease pathology on the prevalence of dementia in the oldest-old. Alzheimers Dement 2016; 12(3): 225-32.

[40] Fiest KM, Roberts JI, Maxwell CJ, *et al.* The prevalence and incidence of dementia due to Alzheimer's Disease: A Systematic Review and Meta-Analysis. Can J Neurol Sci 2016; 43 (Suppl 1): S51-82.

[41] Kojima G, Liljas A, Iliffe S, *et al.* Prevalence of frailty in mild to moderate Alzheimer's Disease: A systematic review and meta-analysis. Curr Alzheimer Res 201; 14(12): 1256-63.

[42] Armijo E, Gonzalez C, Shahnawaz M, *et al.* Increased susceptibility to Abeta toxicity in neuronal cultures derived from familial Alzheimer's disease (PSEN1-A246E) induced pluripotent stem cells. Neurosci Lett 2017; 639: 74-81.

[43] Li K, Wei Q, Liu FF, *et al.* Synaptic dysfunction in Alzheimer's Disease: Abeta, Tau, and epigenetic alterations. Mol Neurobiol 2017.

[44] Schmid S, Jungwirth B, Gehlert V, *et al.* Intracerebroventricular injection of beta-amyloid in mice is associated with long-term cognitive impairment in the modified hole-board test. Behav Brain Res 2017; 324: 15-20.

[45] Kim HY, Lee DK, Chung BR, *et al.* Intracerebroventricular injection of amyloid-beta peptides in normal mice to acutely induce Alzheimer-like cognitive deficits. J Vis Exp 2016; (109).

[46] Choi JG, Moon M, Kim HG, *et al.* Gami-Chunghyuldan ameliorates memory impairment and neurodegeneration induced by intrahippocampal Abeta 1-42 oligomer injection. Neurobiol Learn Mem 2011; 96(2): 306-14.

[47] Christensen R, Marcussen AB, Wortwein G, *et al.* Abeta(1-42) injection causes memory impairment, lowered cortical and serum BDNF levels, and decreased hippocampal 5-HT(2A) levels. Exp Neurol 2008; 210(1): 164-71.

[48] Chai GS, Feng Q, Wang ZH, *et al.* Downregulating ANP32A rescues synapse and memory loss via chromatin remodeling in Alzheimer model. Mol Neurodegener 2017; 12(1): 34.

[49] Trettenbrein PC. The demise of the synapse as the locus of memory: a looming paradigm shift? Front Syst Neurosci 2016; 10: 88.

[50] Jiang Y, Liu Y, Zhu C, *et al.* Minocycline enhances hippocampal memory, neuroplasticity and synapse-associated proteins in aged C57 BL/6 mice. Neurobiol Learn Mem 2015; 121: 20-9.

[51] Xie J, Wang H, Lin T, *et al.* Microglia-Synapse Pathways: Promising therapeutic strategy for alzheimer's disease. Biomed Res Int 2017; 2017: 2986460.

[52] Sell GL, Schaffer TB, Margolis SS. Reducing expression of synapse-restricting protein Ephexin5 ameliorates Alzheimer's-like impairment in mice. J Clin Invest 2017; 127(5): 1646-50.

[53] Nimmrich V, Ebert U. Is alzheimer's disease a result of presynaptic failure? synaptic dysfunctions induced by oligomeric beta-amyloid. Revs Neurosci2009; 20(1): 1-12.

[54] Adlard PA, Bica L, White AR, *et al.* Metal ionophore treatment restores dendritic spine density and synaptic protein levels in a mouse model of Alzheimer's disease. PLoS One 2011; 6(3): e17669.

[55] Potter PE, Rauschkolb PK, Pandya Y, *et al.* Pre- and post-synaptic cortical cholinergic deficits are proportional to amyloid plaque presence and density at preclinical stages of Alzheimer's disease. Acta Neuropathol 2011; 122(1): 49-60.

[56] Scheff SW, Price DA. Alzheimer's disease-related alterations in synaptic density: neocortex and hippocampus. J Alzheimers Dis 2006; 9(3 Suppl): 101-15.

[57] Sze CI, Bi H, Kleinschmidt-DeMasters BK, *et al.* Selective regional loss of exocytotic presynaptic vesicle proteins in Alzheimer's disease brains. J Neurol Sci 2000; 175(2): 81-90.

[58] Tiwari SS, d'Orange M, Troakes C, *et al.* Evidence that the presynaptic vesicle protein CSPalpha is a key player in synaptic degeneration and protection in Alzheimer's disease. Mol Brain 2015; 8: 6.

[59] Koffie RM, Hyman BT, Spires-Jones TL. Alzheimer's disease: Synapses gone cold. Mol Neurodegener 2011; 6(1): 63.

[60] Bezprozvanny I. Calcium signaling and neurodegenerative diseases. Trends Mol Med 2009; 15(3): 89-100.

[61] Popugaeva E, Bezprozvanny I. Role of endoplasmic reticulum Ca^{2+} signaling in the pathogenesis of Alzheimer disease. Front Mol Neurosci 2013; 6: 29.

[62] Zeiger W, Vetrivel KS, Buggia-Prevot V, *et al.* Ca^{2+} influx through store-operated Ca^{2+} channels reduces Alzheimer disease beta-amyloid peptide secretion. J Biol Chem 2013; 288(37): 26955-66.

[63] Giannakopoulos P, Kovari E, Gold G, *et al.* Pathological substrates of cognitive decline in Alzheimer's disease. Front Neurol Neurosci 2009; 24: 20-9.

[64] de Bartolomeis A, Latte G, Tomasetti C, *et al.* Glutamatergic postsynaptic density protein dysfunctions in synaptic plasticity and dendritic spines morphology: Relevance to schizophrenia and other behavioral disorders pathophysiology, and implications for novel therapeutic approaches. Mol Neurobiol 2014, 49(1): 484-511.

[65] Takei Y, Kikkawa YS, Atapour N, *et al.* Defects in synaptic plasticity, reduced NMDA-receptor transport, and instability of postsynaptic density proteins in mice lacking microtubule-associated protein 1A. J Neurosci 2015; 35(47): 15539-54.

[66] Gong Y, Lippa CF. Review: Disruption of the postsynaptic density in Alzheimer's disease and other neurodegenerative dementias. Am J Alzheimers Dis Other Demen 2010; 25(7): 547-55.

[67] Zhou J, Jones DR, Duong DM, *et al.* Proteomic analysis of postsynaptic density in Alzheimer's disease. Clin Chim Acta 2013 420: 62-8.

[68] Li F, Wu X, Li J, *et al.* Ginsenoside Rg1 ameliorates hippocampal long-term potentiation and memory in an Alzheimer's disease model. Mol Med Rep 2016; 13(6): 4904-10.

[69] Qi X, Zhang K, Xu T, *et al.* Sex differences in long-term potentiation at Temporoammonic-CA1 synapses: Potential implications for memory consolidation. PLoS One 2016; 11(11): e0165891.

[70] Andrade-Talavera Y, Benito I, Casanas JJ, *et al.* Rapamycin restores BDNF-LTP and the persistence of long-term memory in a model of Down's syndrome. Neurobiol Dis 2015; 82: 516-25.

[71] Yang Q, Zhu G, Liu D, *et al.* Extrasynaptic NMDA receptor dependent long-term potentiation of hippocampal CA1 pyramidal neurons. Sci Rep 2017; 7(1): 3045.

[72] Huh S, Baek SJ, Lee KH, *et al.* The reemergence of long-term potentiation in aged Alzheimer's disease mouse model. Sci Rep 2016; 6: 29152.

[73] Wu Z, Guo Z, Gearing M, *et al.* Tonic inhibition in dentate gyrus impairs long-term potentiation and memory in an Alzheimer's [corrected] disease model. Nat Commun 2014, 5: 4159.

[74] Huang SH, Wang J, Sui WH, *et al.* BDNF-dependent recycling facilitates TrkB translocation to postsynaptic density during LTP *via* a Rab11-dependent pathway. J Neurosci 2013; 33(21): 9214-30.

[75] Panja D, Kenney JW, D'Andrea L, *et al.* Two-stage translational control of dentate gyrus LTP consolidation is mediated by sustained BDNF-TrkB signaling to MNK. Cell Rep 2014; 9(4): 1430-45.

[76] Motaghinejad M, Motevalian M, Babalouei F, *et al.* Possible involvement of CREB/BDNF signaling pathway in neuroprotective effects of topiramate against methylphenidate induced apoptosis, oxidative stress and inflammation in isolated hippocampus of rats: Molecular, biochemical and histological evidences. Brain Res Bull 2017, 132: 82-98.

[77] Alzoubi KH, Alkadhi KA. Chronic Nicotine Treatment Reverses Hypothyroidism-Induced Impairment of L-LTP Induction Phase: Critical Role of CREB. Molecular Neurobiology 2014; 49(3): 1245-55.

[78] Bridi MS, Hawk JD, Chatterjee S, *et al*. Pharmacological activators of the NR4A nuclear receptors enhance LTP in a CREB/CBP-dependent manner. Neuropsychopharmacology 2017; 42(6): 1243-53.

[79] Corbett GT, Roy A, Pahan K. Sodium phenylbutyrate enhances astrocytic neurotrophin synthesis via protein kinase C (PKC)-mediated activation of cAMP-response element-binding protein (CREB): Implications for Alzheimer disease therapy. J Biol Chem 2013; 288(12): 8299-312.